Symmetric mass generation of interacting chiral fermions on a one-dimensional lattice without fermion doubling

V. A. Zakharov,[1,*] Atsushi Ueda,[2,*] Frank Verstraete,[2,3] and C. W. J. Beenakker[1]

[1] *Instituut-Lorentz, Universiteit Leiden, P.O. Box 9506, 2300 RA Leiden, The Netherlands*
[2] *Department of Physics and Astronomy, Ghent University, Krijgslaan 281, 9000 Gent, Belgium*
[3] *Department of Applied Mathematics and Theoretical Physics, University of Cambridge, Wilberforce Road, Cambridge, CB3 0WA, United Kingdom*

(Dated: June 2026)

Symmetric mass generation is the interaction-induced opening of a fermion gap without spontaneous symmetry breaking. The anomaly-free 3–4–5–0 model of Wang and Wen provides a minimal one-dimensional setting for this phenomenon, but a direct lattice realization faces two obstacles: fermion doubling for local chiral discretizations and perturbative irrelevance of the six-fermion gapping interaction. We address both obstacles. First, we formulate the model on a strictly one-dimensional tangent-fermion lattice, where a nonlocal hopping produces a single chiral branch without a mirror partner while retaining an efficient tensor-network representation. Second, we add a Hubbard-type density-density interaction (Luttinger parameter K) that reduces the scaling dimension of the 3–4–5–0 interaction from 5 to $5K$, making it relevant for $K < 2/5$. Density-matrix renormalization group calculations show the opening of an excitation gap in this regime without the appearance of a degenerate ground state, the hallmark of symmetric mass generation.

I. INTRODUCTION

Massless fermions provide an idealized framework for the exploration of strongly interacting quantum systems, both in condensed matter [1–3] and in particle physics [4–6]. In one spatial dimension (1D) they are characterized by a linear dispersion relation and a definite chirality, either left-moving or right-moving. The edge of a quantum Hall insulator provides a condensed-matter realization of 1D chiral fermions, with a quantized electrical conductance $G_{\rm H}$ and thermal conductance $G_{\rm T}$.

The zero-mass property is protected by internal symmetries which prevent the coupling of left-movers and right-movers that would gap the spectrum. Strong interactions can generate a mass by spontaneous symmetry breaking (the Anderson-Higgs mechanism [7]), but there may be an alternative: *symmetric mass generation* (SMG) — a process by which interactions produce mass while preserving the underlying symmetries [8–11].

A necessary condition for SMG to work is that the fermions are anomaly-free [12]. In the quantum Hall context this means that both $G_{\rm H}$ and $G_{\rm T}$ should vanish. This condition restricts the number $N_{\rm L}$ and $N_{\rm R}$ of left-movers and right-movers, and their integer charges q_n, since $G_{\rm H} \propto \sum_{i\in{\rm L}} q_i^2 - \sum_{j\in{\rm R}} q_j^2$ and $G_{\rm T} \propto N_{\rm L} - N_{\rm R}$.

The 3–4–5–0 model introduced by Wang and Wen [13, 14] is a test ground for SMG of 1D chiral fermions: There are two right-movers, with charges 3 and 4, and two left-movers, with charges 5 and 0, so the model is anomaly-free ($N_{\rm L} = N_{\rm R}$ and $3^2 + 4^2 = 5^2 + 0^2$, see Fig. 1). The charges are co-prime, a mass term that gaps the spectrum by coupling left-movers and right-movers is prohibited by the U(1) symmetry responsible for charge conservation.

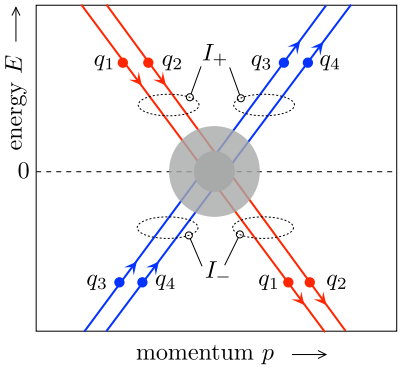

FIG. 1. Dispersion of 1D chiral fermions, consisting of two branches of left-moving fermions (charges q_1 and q_2) and two branches of right-moving fermions (charges q_3 and q_4). Arrows indicate the spectral flow induced by an electric field F. If the negative energy branches are decoupled from the positive energy branches by a gap in the shaded energy-momentum region, the net charge current density I_- that flows from negative energy into this region should vanish. One has $I_- = \sum_n {\rm sign}(v_n) q_n^2 (F/h)$, with $v_n = dE_n/dp$ the velocity in mode n. In the 3–4–5–0 model the gap condition $I_- = 0$ is fulfilled by choosing $q_1 = 5$, $q_2 = 0$, $q_3 = 3$, $q_4 = 4$.

Zeng *et al.* [15] demonstrated the interaction-induced gap opening in the 3–4–5–0 model on a 2D lattice (2+1 dimensional space-time). The additional spatial dimension was needed to accommodate the mirror fermions that appear for any local, chirality-preserving discretization of the Hamiltonian [16]. A fine-tuning of the hopping matrix elements decouples the mirror fermions so that their system is effectively 1D.

Recently, related one-dimensional or exactly solvable approaches with local infinite-dimensional Hilbert spaces to anomaly-free chiral lattice gauge theories have also been proposed using emergent translation symmetry,

* These two authors contributed equally.

symmetry disentanglers, modified Villain Hamiltonians and Euclidean models [17–24].

Here we demonstrate SMG on a strictly 1D lattice. By working with Stacey's nonlocal discretization of the Hamiltonian [25] (with a tangent rather than a sine dispersion) we circumvent the fermion-doubling obstruction and enable the study of SMG in a minimally constrained setting. Our "tangent fermion" formulation builds on recent advances in quantum Monte Carlo [26] and density-matrix renormalization group (DMRG) methods [27–29], that preserve computational efficiency by exploiting the fact that the nonlocal Hamiltonian corresponds to a *local* generalized eigenvalue problem [30].

The restriction from 2D to 1D is one way in which this study goes beyond Ref. 15. The second way is that we work around a complication of the 3–4–5–0 model, that the gapping interaction is irrelevant in the sense of the renormalization group (RG). To allow an RG scaling analysis to reliably guide the numerics, we need to make the gapping interaction relevant. Here we achieve that by introducing an additional Hubbard-type density-density interaction, which reduces the scaling dimension of the gapping interaction and makes it perturbatively relevant for Luttinger parameter $K < 2/5$. The result is a controlled setting in which the interaction responsible for SMG is the same anomaly-free 3–4–5–0 interaction, while the auxiliary Hubbard term only tunes its scaling dimension. This separates the origin of the gap from the mechanism that makes the gapping perturbation visible at accessible system sizes.

The outline of the paper is as follows. In Secs. II and III we present the two key ingredients of our work: We first formulate the 3–4–5–0 model on a 1D lattice without fermion doubling and then make the 3–4–5–0 interaction RG relevant by adding a Hubbard repulsion. All of this is informed by the bosonization analysis of Sec. IV. Our DMRG results are presented in Sec. V, focusing on the hallmark of symmetric mass generation: the opening of an excitation gap while keeping the ground state nondegenerate. We conclude in Sec. VI.

II. 3–4–5–0 TANGENT FERMIONS

The 3–4–5–0 model [13, 14] on a 1D lattice (unit lattice constant) has Hamiltonian $H = H_0 + H_{3450}$, consisting of the free fermion part

$$H_0 = \sum_{n>m} t_{nm}\big(c^\dagger_{n,3}c_{m,3} + c^\dagger_{n,4}c_{m,4} - c^\dagger_{n,5}c_{m,5} - c^\dagger_{n,0}c_{m,0}\big) + \text{H.c.}, \tag{2.1}$$

with hopping matrix elements t_{nm}, and the interacting part

$$H_{3450} = \sum_n \big(g_1 c_{n,3}c^\dagger_{n,4}c^\dagger_{n+1,4}c_{n,5}c_{n,0}c_{n+1,0} + g_2 c_{n,3}c_{n+1,3}c_{n,4}c^\dagger_{n,5}c^\dagger_{n+1,5}c_{n,0}\big) + \text{H.c.}, \tag{2.2}$$

with coupling constants $g_1, g_2 > 0$. The indices of the fermionic operators $c_{n,\alpha}$ indicate the lattice site $n \in \mathbb{Z}$ and the charge $\alpha \in \{3, 4, 5, 0\}$. (We set the electron charge e and $\hbar$ equal to unity.)

The nearest-neighbor hopping $t_{nm} = (t_0/2i)\delta_{n,m+1}$ produces the sine dispersion $E(k) = t_0 \sin k$, with a spurious mirror fermion at $k = \pi$. To avoid this fermion doubling we adopt Stacey's long-range hopping [25]

$$t_{nm} = 2it_0(-1)^{n-m}, \tag{2.3}$$

corresponding to the tangent dispersion $E(k) = 2t_0 \tan(k/2)$. The highly nonlocal "all-to-all" coupling (2.3) becomes a local coupling if the Schrödinger equation $H\psi = E\psi$ is reformulated as a generalized eigenvalue problem $P\psi = EQ\psi$, with Hermitian operators P, Q that only couple nearby lattice sites [30]. One can thus work around the fermion-doubling obstruction without compromising computational efficiency [31].

Since $\tan(k/2)$ has a positive slope in the Brillouin zone $|k| < \pi$, the fermions with charge 3 and 4 in Eq. (2.2) are right-movers, while the fermions with charge 5 and 0 are left-movers. The pair of six-fermion interaction terms $\propto g_1, g_2$ conserve charge (at the origin of the U(1) symmetry),

$$\sum_\alpha q_\alpha \ell_\alpha = 0, \tag{2.4}$$

where $\ell_\alpha \in \mathbb{Z}$ counts how many fermion operators of charge α appear in the interaction term (positive ℓ_α for a creation operator, negative ℓ_α for an annihilation operator).

Necessary conditions for an interaction-induced mass are that there are $N_\text{L} = N_\text{R}$ interaction terms, with linearly independent interaction vectors $\boldsymbol{\ell}^{(p)}$ that satisfy the null condition [32–35]

$$\sum_\alpha \text{sign}(v_\alpha)\ell^{(p)}_\alpha \ell^{(p')}_\alpha = 0, \quad \text{for all } \ p, p'. \tag{2.5}$$

The Hamiltonian (2.2) has interaction vectors

$$\begin{aligned} \boldsymbol{\ell}^{(1)} &= (1, -2, 1, 2), \\ \boldsymbol{\ell}^{(2)} &= (2, 1, -2, 1), \end{aligned} \tag{2.6}$$

for $\boldsymbol{q} = (3, 4, 5, 0)$, so that both conditions (2.4) and (2.5) are satisfied.

We note that the charges do not uniquely follow from the interaction vectors. For example, charges 7–11–13–1 also satisfy the charge conservation rule (2.4). We also note that the anomaly-free condition

$$\sum_\alpha \text{sign}(v_\alpha) q_\alpha^2 = 0 \tag{2.7}$$

is not an independent condition on the charges once the interaction vectors are given — Eq. (2.7) follows algebraically from Eqs. (2.4) and (2.5).

III. SMG AT WEAK COUPLING ENABLED BY HUBBARD REPULSION

A. Renormalized scaling dimension

We recall the basics of the scaling analysis of interacting fermions [36]. Interactions can open a gap in the spectrum of an infinite 1+1 dimensional system if the scaling dimension $D < 2$. If $D > 2$ the interactions are irrelevant, the system scales to the free-fermion limit when the size tends to infinity.

In the non-interacting limit, the six-fermion interaction (2.2) has scaling dimension

$$D_{3450} = \tfrac{1}{2}|\boldsymbol{\ell}^{(p)}|^2 = 5, \tag{3.1}$$

and is therefore highly irrelevant. Strong coupling, however, may renormalize the scaling dimension, such that H_{3450} becomes relevant and opens a gap in a deeply nonperturbative regime. This is the approach taken previously in Ref. 15.

Here, we take a different route: we keep the six-fermion interaction at moderately weak coupling, where an RG scaling analysis reliably guides the numerical simulations. We add an on-site Hubbard-type density-density interaction, a four-fermion interaction that couples the density of left-movers and right-movers,

$$\begin{aligned} H_{\text{Hubbard}} &= U_{\text{H}} \sum_n (\nu_3 \delta\rho_{n,3} + \nu_4 \delta\rho_{n,4}) \\ &\quad \times (\nu_5 \delta\rho_{n,5} + \nu_0 \delta\rho_{n,0}), \qquad (3.2a) \\ \delta\rho_{n,\alpha} &= c^\dagger_{n,\alpha} c_{n,\alpha} - \langle c^\dagger_{n,\alpha} c_{n,\alpha}\rangle, \qquad (3.2b) \end{aligned}$$

with weight factors ν_α. As the Hamiltonian H_{Hubbard} causes no backscattering, it cannot open a gap. Nonetheless, it can modify the scaling dimension of H_{3450} and thereby enable a gap opening at weak coupling.

The bosonization analysis in Sec. IV shows that if we choose the weight factors according to the interaction vectors, $(\nu_3, \nu_4, \nu_5, \nu_0) = \boldsymbol{\ell}^{(p)}$, so that the Hubbard interaction takes the form

$$\begin{aligned} H_{\text{Hubbard}} &= \sum_n U_n, \qquad (3.3a) \\ U_n &= -U^{(1)}_{\text{H}} (\delta\rho_{n,3} - 2\delta\rho_{n,4})(\delta\rho_{n,5} + 2\delta\rho_{n,0}) \\ &\quad - U^{(2)}_{\text{H}} (2\delta\rho_{n,3} + \delta\rho_{n,4})(-2\delta\rho_{n,5} + \delta\rho_{n,0}), \qquad (3.3b) \end{aligned}$$

that with this choice of weights, the scaling dimensions $D^{(1)}_{3450}, D^{(2)}_{3450}$ of the g_1 and g_2 terms in H_{3450} can be *independently* tuned by a pair of effective Luttinger parameters K_1, K_2, according to

$$\begin{aligned} &D^{(\alpha)}_{3450} = 5K_\alpha, \quad K_\alpha = \sqrt{\frac{2\pi t_0 - C U^{(\alpha)}_{\text{H}}}{2\pi t_0 + C U^{(\alpha)}_{\text{H}}}}, \\ &C = \sqrt{\nu_3^2 + \nu_4^2}\sqrt{\nu_5^2 + \nu_0^2} = 5. \end{aligned} \tag{3.4}$$

In the following, we set $g_1 = g_2$, $U^{(1)}_{\text{H}} = U^{(2)}_{\text{H}} \equiv U_{\text{H}} > 0$, $K_1 = K_2 \equiv K \in (0,1)$. The 3–4–5–0 interaction then becomes relevant for $K < 2/5 \equiv K_c$.

B. Elimination of Friedel oscillations

At nonzero Fermi wave vector k_{F} the electron density correlators have rapid Friedel oscillations $\propto e^{ik_{\text{F}}x}$, that reduce the effectiveness of the gap opening interactions. To eliminate these we proceed as follows.

We denote by N_α the expectation value of the number of fermions of charge α relative to a half-filled band (the free-fermion vacuum). The corresponding Fermi wave vector k_α is

$$k_\alpha = (2\pi/L)\,\text{sign}(v_\alpha) N_\alpha. \tag{3.5}$$

Friedel oscillations in the correlators are absent if

$$\begin{aligned} &\sum_\alpha \ell^{(p)}_\alpha k_\alpha = 0 \Rightarrow \mathcal{N}^{(p)} = 0, \ \text{ for all } \ p, \\ &\text{with } \ \mathcal{N}^{(p)} = \sum_\alpha \text{sign}(v_\alpha) \ell^{(p)}_\alpha N_\alpha. \end{aligned} \tag{3.6}$$

The Hamiltonian H_{3450} conserves charge but not particle number. We can therefore not enforce $N_\alpha \equiv 0$ (half-filled band for each charge), to satisfy Eq. (3.6). Instead, setting $\mathcal{N}^{(p)} \equiv 0$ for all p is permitted because $\mathcal{N}^{(p)}$ is conserved by H_{3450}.

To see this, we note that N_α can change due to the interactions by an amount $\delta N_\alpha = \sum_p n^{(p)} \ell^{(p)}_\alpha$ with $n^{(p)} \in \mathbb{Z}$. The corresponding change in $\mathcal{N}^{(p)}$ is

$$\delta\mathcal{N}^{(p)} = \sum_{p'} n^{(p')} \sum_\alpha \text{sign}(v_\alpha) \ell^{(p)}_\alpha \ell^{(p')}_\alpha = 0, \tag{3.7}$$

in view of the null condition (2.5).

IV. BOSONIZATION ANALYSIS

A. Charge rotation decouples the Luttinger liquid

At first sight, the lattice model introduced in Sec. II appears rather complicated. Its interactions mix the four fermion flavors in a nontrivial way, and it is therefore not immediately obvious why these particular terms preserve the symmetry required for symmetric mass generation. The structure becomes more transparent after bosonization of the low-energy theory.

We begin with the noninteracting Hamiltonian (2.1). The four chiral fermions are represented by chiral bosonic fields $\varphi_{qR/L}$, where q denotes the charge and R/L the chirality (charges 3,4 right-moving, charges 5,0 left-moving).

The free Hamiltonian is

$$H_{\rm free} = \frac{1}{4\pi}\int dx\,\left[(\partial_x\varphi_{3R})^2 + (\partial_x\varphi_{4R})^2 + (\partial_x\varphi_{5L})^2 + (\partial_x\varphi_{0L})^2\right] = \frac{1}{4\pi}\int dx\,\left[(\partial_x\Phi_R)^2 + (\partial_x\Phi_L)^2\right], \tag{4.1}$$

(4.2)

where we have collected the chiral fields in vectors

$$\Phi_R = (\varphi_{3R},\varphi_{4R}),\quad \Phi_L = (\varphi_{5L},\varphi_{0L}),\quad \Phi = (\Phi_R,\Phi_L). \tag{4.3}$$

The free Hamiltonian is invariant under independent orthogonal rotations of the right-moving and left-moving fields,

$$\widetilde{\Phi}_R = Q_R\Phi_R, \qquad \widetilde{\Phi}_L = Q_L\Phi_L. \tag{4.4}$$

We will use this transformation to isolate neutral modes from charged modes. Similar changes of basis have been used, for example, in the study of conformal boundary conditions [38–40].

We take

$$Q_R = \frac{1}{\sqrt{5}}\begin{pmatrix}1 & -2\\ 2 & 1\end{pmatrix}, \qquad Q_L = -\frac{1}{\sqrt{5}}\begin{pmatrix}1 & 2\\ -2 & 1\end{pmatrix}, \tag{4.5}$$

chosen such that

$$\boldsymbol{\ell}^{(p)} = \sqrt{5}\left([Q_R]_{p,1},[Q_R]_{p,2},-[Q_L]_{p,1},-[Q_L]_{p,2}\right), \tag{4.6}$$

see Eq. (2.6).

With this choice,

$$\boldsymbol{\ell}^{(p)}\Phi = 2\sqrt{5}\,\phi_p, \tag{4.7}$$

where we have introduced the nonchiral two-component bosonic fields

$$\phi = \tfrac{1}{2}(\widetilde{\Phi}_R - \widetilde{\Phi}_L), \qquad \theta = \tfrac{1}{2}(\widetilde{\Phi}_R + \widetilde{\Phi}_L). \tag{4.8}$$

The free Hamiltonian then decomposes into two decoupled Tomonaga-Luttinger liquids [41–43],

$$H_{\rm free} = \sum_{p=1}^{2}\frac{v}{2\pi}\int dx\,\left[K_p(\partial_x\theta_p)^2 + \frac{1}{K_p}(\partial_x\phi_p)^2\right], \tag{4.9}$$

with $K_p = v = 1$ at the free-fermion point.

The change of basis makes the charge symmetry explicit. A global U(1) charge rotation acts on the fermions as

$$c_q \mapsto e^{iq\chi}c_q, \tag{4.10}$$

and therefore shifts the bosonic fields according to

$$\Phi_\alpha \mapsto \Phi_\alpha + \chi q_\alpha. \tag{4.11}$$

Eq. (4.5) then gives

$$\phi_p \mapsto \phi_p,\quad \theta_1 \mapsto \theta_1 - \sqrt{5}\,\chi,\quad \theta_2 \mapsto \theta_2 + 2\sqrt{5}\,\chi. \tag{4.12}$$

Thus the fields θ are charged, while the fields ϕ are neutral.

Vertex operators built from the charged field θ are forbidden by charge conservation, while vertex operators built from the neutral field ϕ are allowed, and can be used to introduce the 3–4–5–0 interaction. The lowest-order local vertex operators are

$$V_p = \cos(\boldsymbol{\ell}^{(p)}\Phi) = \cos(2\sqrt{5}\,\phi_p),\quad p = 1,2. \tag{4.13}$$

After re-fermionization, $c_{x,q} \sim e^{i\varphi_q(x)}$, these are precisely the two six-fermion operators in the 3–4–5–0 interaction (2.2).

The scaling dimension of an interaction $\propto \cos\beta\phi_p$ is $\beta^2K_p/4$, so for V_p this is $5K_p$. For $K_p < 2/5$ the cosine interaction is relevant and can pin the field ϕ_p to a local minimum, gapping out the fermionic excitations. When both cosines are relevant, $K_1, K_2 < 2/5$, both Luttinger liquids are gapped. Since the pinned fields are invariant under the charge rotation (4.12), this gap opening does not break the protecting U(1) symmetry.

B. Scaling dimension

We next identify the density-density interaction that reduces the scaling dimension of the operators V_p. In view of Eq. (4.9), a reduction of K_p is produced by the interaction

$$\mathcal{O}_p = (\partial_x\theta_p)^2 - (\partial_x\phi_p)^2 = \partial_x\widetilde{\varphi}_{L,p}\,\partial_x\widetilde{\varphi}_{R,p}. \tag{4.14}$$

Upon refermionization, $\partial_x\varphi_q(x) \mapsto \mathrm{sign}(v_q)\delta\rho_{x,q}$, this interaction becomes the Hubbard-type density-density interaction (3.3). It couples left-moving and right-moving densities, but it does not backscatter the chiral fermions and therefore does not by itself open a gap. Its role is instead to renormalize the free-fermion scaling dimension $D_{3450} = 5$ by

$$D^{(p)}_{3450} = 5K_p. \tag{4.15}$$

The 3–4–5–0 interaction becomes relevant once $K_p < 2/5$, which is the criterion used to guide the numerical simulations.

C. Gapping without emergent ground state degeneracy

A distinctive feature of gapping by the SMG mechanism is that the ground state remains nondegenerate. Because this will play a key role in the interpretation of our numerics, we explain it in some detail.

The four components of the chiral bosonic field Φ are defined modulo 2π, the field is compactified on the four-torus $\mathbb{T}^4$. We define the map $\mathcal{A}$ from $\mathbb{T}^4$ to $\mathbb{T}^2$ by

$$\mathcal{A}\Phi = A\Phi \bmod 2\pi,\quad A = \begin{pmatrix}1 & -2 & 1 & 2\\ 2 & 1 & -2 & 1\end{pmatrix}. \tag{4.16}$$

The two rows of A are the interaction vectors $\boldsymbol{\ell}^{(1)}$ and $\boldsymbol{\ell}^{(2)}$, so that

$$[A\Phi]_p = \boldsymbol{\ell}^{(p)}\Phi = 2\sqrt{5}\,\phi_p. \tag{4.17}$$

The map $\mathcal{A}$ covers the whole of $\mathbb{T}^2$ (it is surjective), because it can generate the two basis states of the two-torus:

$$A(0,1,1,1)^\top = \binom{1}{0}, \quad A(1,1,1,0)^\top = \binom{0}{1}. \tag{4.18}$$

Without loss of generality [44] we may choose the sign of the couplings such that the cosine potential minima are located at $\boldsymbol{\ell}^{(p)}\Phi = 0 \bmod 2\pi$, $p = 1, 2$. Its pre-image

$$\mathcal{M} = \{x \in \mathbb{T}^4 : Ax = 0 \bmod 2\pi\} \tag{4.19}$$

is the kernel of the map $\mathcal{A}$.

The pinned ground state is nondegenerate if $\mathcal{M}$ is singly connected on $\mathbb{T}^4$. It is a basic theorem of algebraic geometry [45] that the kernel of a surjective integer-matrix map between tori has a number of connected components equal to the greatest common divisor (gcd) of the set of maximal minors of the matrix. Since A is a 2×4 matrix, its maximal minors are the determinants of its six 2×2 submatrices. Columns 1 and 2 have gcd 5, columns 2 and 3 have gcd 3, so this already fixes the gcd of all minors at 1 and we conclude that $\mathcal{M}$ has only a single connected component.

An equivalent way to state this algebraic result is that the ground state is nondegenerate because the lattice of interaction vectors,

$$\Lambda = \mathrm{span}_{\mathbb{Z}}\{\boldsymbol{\ell}^{(1)}, \boldsymbol{\ell}^{(2)}\} \subset \mathbb{Z}^4 \tag{4.20}$$

is primitive [46]. The primitivity condition means that there is no allowed local vertex operator whose exponent is a nontrivial fractional linear combination of the pinned fields. In particular, $\boldsymbol{\ell}^{(p)}/2 \notin \mathbb{Z}^4$, so the half-harmonics $\cos(\boldsymbol{\ell}^{(p)}\Phi/2)$ and $\sin(\boldsymbol{\ell}^{(p)}\Phi/2)$ are not operators in the fermionic Hilbert space.

This is the essential difference from an ordinary symmetry-breaking sine-Gordon problem, with a non-primitive pinning potential $\cos(2m\Phi)$. The minima $m\Phi = 0$ and $m\Phi = \pi$ are not related by the compactification of the bosonic fields and can be distinguished by the local order parameter $\cos(m\Phi)$. As demonstrated for the tangent fermion Luttinger liquid in Ref. 29, this produces a degenerate ground-state manifold, accompanied by spontaneous symmetry breaking.

V. RESULTS

We consider two related signatures of symmetric mass generation: firstly in the excitation spectrum, secondly in the occupation factor. We then show numerical DMRG results on tensor networks (see App. A) that exhibit both signatures.

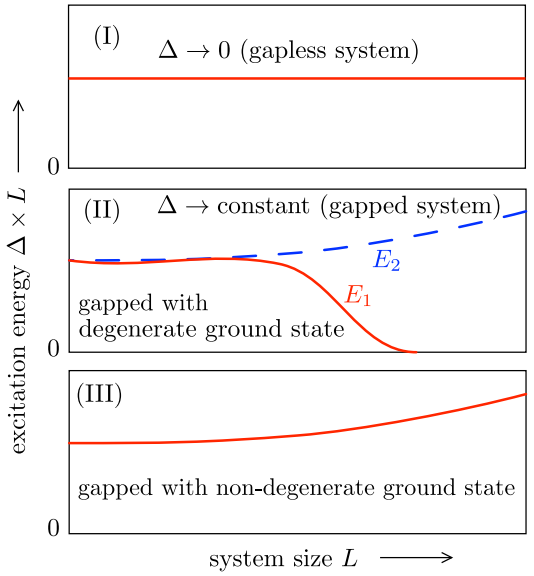

FIG. 2. Comparison of the expected dependence on the system size L of the excitation energy Δ (energy of an excited state relative to the ground state). Panel I shows the finite-size gap $\Delta \propto 1/L$ in a system that is gapless in the thermodynamic limit (a flat line when $\Delta \times L$ is plotted versus L). Panels II and III compare a gapped system with (II) or without (III) the appearance of a degenerate ground state. In case II, the symmetry is broken when E_1 merges with the ground state, leaving a gap to the next level E_2. Case III represents symmetric mass generation (SMG).

A. Excitation gap

Our goal is to distinguish three types of infinite-system spectra from finite-size data: (I) a gapless system; (II) a gapped system with broken U(1) symmetry; (III) a gapped system with preserved U(1) symmetry. The presence of a finite-size gap $\Delta = \hbar v/L$ in a system of size L complicates the distinction. In Fig. 2 we illustrate what we expect for the L-dependence of the excitation gap in each of the three cases.

Case (I) is distinguished by the $1/L$ decay of the energy of the lowest excited state (relative to the ground state). In both cases (II) and (III) an excitation gap remains in the large-L limit; the distinguishing feature is that in case (II) the lowest excited state E_1 merges with the ground state and the gap refers to the energy of the next level E_2. The appearance of a degenerate ground state is the signature of the Higgs mechanism for mass generation via spontaneously broken symmetry, see Ref. 29 for a tangent fermion realization.

The DMRG results in Fig. 3d) show the expected case III spectrum, indicative of SMG. The four panels isolate the two ingredients of the construction. For $g_1 = g_2 = 0$, the Hubbard interaction changes the Luttinger parameter but does not by itself produce the SMG gap. In contrast, for $K > K_c$, the 3–4–5–0 interaction remains irrelevant, and the spectrum retains the finite-size behav-

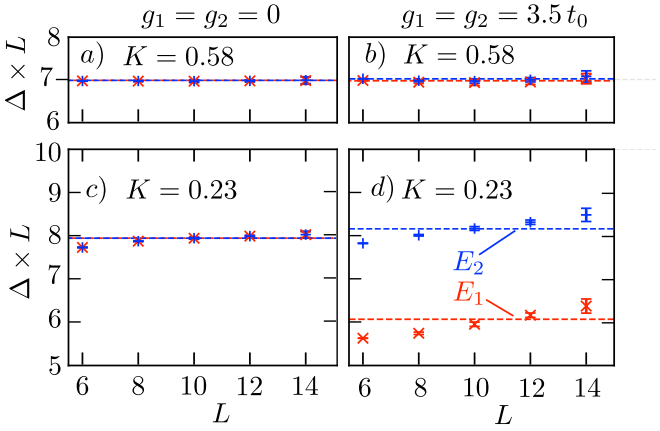

FIG. 3. DMRG results for the energies of the two lowest excited states E_1, E_2 (measured relative to the ground state), of tangent fermions in the 3–4–5–0 model on an L-site 1D lattice (anti-periodic boundary conditions, bond dimension $\chi_{\rm MPS} = 16384$). Data points with error bars (see App. A 2) are the numerical results, the dashed line is what we would expect for a gapless system (case I in Fig. 2). A gap opening without a degenerate ground state (case III) appears in panel *d)* in the presence of both the 3–4–5–0 interaction ($g_1 = g_2 = 3.5$) and a sufficiently strong Hubbard interaction ($K < 2/5$).

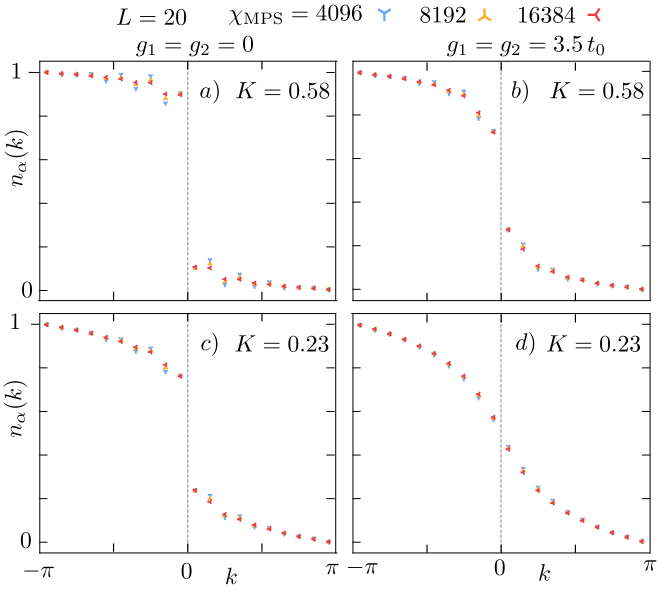

FIG. 4. DMRG results for the momentum dependent occupation factor $n_\alpha(k)$ of a right-moving charge (equivalently, $\alpha = 3$ or 4), computed for $L = 20$ at three different MPS bond dimensions $\chi_{\rm MPS}$. The four panels correspond to the four panels in Fig. 3. The steep rise near $k = 0$ is smoothed in panel *d)*.

ior expected of a gapless system. Only when the 3–4–5–0 interaction is combined with a sufficiently small Luttinger parameter, $K < K_c$, do the two lowest excitation energies separate from the gapless scaling line without an accompanying collapse of E_1 onto the ground state. This is the finite-size signature expected for a symmetric, rather than symmetry-breaking, mass generation mechanism.

B. Occupation factor

The occupation factor $n_\alpha(k)$, the Fourier transform of the charge-α propagator $C_\alpha(x) = \langle c_\alpha^\dagger(x) c_\alpha(0)\rangle$, has a power-law singularity at $k = 0$ for a gapless Luttinger liquid [36],

$$n_\alpha(k) \propto |k|^{[K+K^{-1}]/2-1}. \tag{5.1}$$

For a gapped system, instead, a smooth k-dependence follows from the exponential decay of the propagator.

In a finite system, the discreteness of k removes the singularity, but a steep rise remains in a gapless system, as can be seen in Fig. 4, panels a,b,c). The steep rise is smoothed in panel d), consistent with the gap data from Fig. 3.

VI. CONCLUSION

We have studied symmetric mass generation (SMG) in the anomaly-free 3–4–5–0 model [13, 14] on a strictly one-dimensional lattice, employing fermions with a tangent dispersion ("tangent fermions") as an alternative to lattice constructions [15] in which the unwanted mirror fermions are accommodated in an additional spatial dimension. To make the SMG mechanism visible in a weak-coupling scaling regime, we introduced a Hubbard-type density-density interaction that renormalizes the Luttinger parameter K, reducing the scaling dimension. For $K < K_c = 2/5$, the gap-opening interaction becomes relevant.

The DMRG results exhibit the expected finite-size signatures of this mechanism. When either the 3–4–5–0 interaction or the sufficiently strong Hubbard renormalization is absent, the low-lying spectrum follows the behavior expected of a gapless system. When both are present, the excitation spectrum develops a gap while the ground state remains nondegenerate. The momentum occupation factor shows the corresponding smoothing of the Luttinger-liquid singularity. Taken together, these observations are consistent with interaction-induced mass generation without spontaneous breaking of the protecting U(1) symmetry.

The tangent-fermion formalism realizes each chiral fermion flavor directly and independently on the lattice. This provides a useful framework in which the bosonization dictionary is particularly transparent. Indeed, this transparency was essential for identifying the Hubbard interaction in the simple form used here. We therefore expect tangent fermions to be useful more broadly in future studies of strongly interacting chiral fermions and their dynamics.

ACKNOWLEDGMENTS

Figure 1 was suggested to us by S. Polla. AU thanks L. Lootens for helpful discussions. Data sets are available at a Zenodo repository.
Research in Leiden was supported by the Netherlands Organisation for Scientific Research (NWO/OCW), as part of Quantum Limits (project number SUMMIT.1.1016). AU was supported by BOF-GOA (Grant No. BOF23/GOA/021) and by FWO Junior Postdoctoral Fellowship (grant No. 3E0.2025.0049.01). FV acknowledges funding from the UKRI (EP/Z003342/1), EOS (40007526) and IBOF (IBOF23/064).

Appendix A: DMRG calculation

1. MPO representation

For the DMRG calculation we need to represent the Hamiltonian as a matrix-product operator (MPO) [47], a product of matrices $M^{(n)}$ that act only on site n. The calculation is efficient if the dimension of each matrix (the MPO bond dimension $\chi_{\rm MPO}$) is independent of the number of lattice sites N. Such a scale independent MPO is possible for short-range hoppings, and also for long-range hoppings that correspond to a local generalized eigenvalue problem [28].

The free tangent fermion Hamiltonian (2.1) has MPO representation

$$H_0 = [M_0^{(1)} M_0^{(2)} \cdots M_0^{(N)}]_{1,10} \tag{A1}$$

with bond-dimension 10 matrices

$$M_0^{(n)} = \begin{pmatrix} 1 & c_{n,3} & c_{n,3}^\dagger & c_{n,4} & c_{n,4}^\dagger & c_{n,5} & c_{n,5}^\dagger & c_{n,0} & c_{n,0}^\dagger & (2it_0)^{-1}U_n \\ 0 & -1 & 0 & 0 & 0 & 0 & 0 & 0 & 0 & 2it_0 c_{n,3}^\dagger \\ 0 & 0 & -1 & 0 & 0 & 0 & 0 & 0 & 0 & 2it_0 c_{n,3} \\ 0 & 0 & 0 & -1 & 0 & 0 & 0 & 0 & 0 & 2it_0 c_{n,4}^\dagger \\ 0 & 0 & 0 & 0 & -1 & 0 & 0 & 0 & 0 & 2it_0 c_{n,4} \\ 0 & 0 & 0 & 0 & 0 & -1 & 0 & 0 & 0 & -2it_0 c_{n,5}^\dagger \\ 0 & 0 & 0 & 0 & 0 & 0 & -1 & 0 & 0 & -2it_0 c_{n,5} \\ 0 & 0 & 0 & 0 & 0 & 0 & 0 & -1 & 0 & -2it_0 c_{n,0}^\dagger \\ 0 & 0 & 0 & 0 & 0 & 0 & 0 & 0 & -1 & -2it_0 c_{n,0} \\ 0 & 0 & 0 & 0 & 0 & 0 & 0 & 0 & 0 & 1 \end{pmatrix}. \tag{A2}$$

We have also included the Hubbard interaction (3.3), which is purely on-site so it does not change the bond dimension. The 3–4–5–0 interaction (2.2) has bond dimension 6,

$$H_{3450} = [M_{3450}^{(1)} M_{3450}^{(2)} \cdots M_{3450}^{(N)}]_{1,6}, \tag{A3}$$

$$M_{3450}^{(n)} = \begin{pmatrix} 1 & c_{n,3}c_{n,4}^\dagger c_{n,5}c_{n,0} & c_{n,0}^\dagger c_{n,5}^\dagger c_{n,4}c_{n,3}^\dagger & c_{n,3}c_{n,4}c_{n,5}^\dagger c_{n,0} & c_{n,0}^\dagger c_{n,5}c_{n,4}^\dagger c_{n,3}^\dagger & 0 \\ 0 & 0 & 0 & 0 & 0 & g_1 c_{n,4}^\dagger c_{n,0} \\ 0 & 0 & 0 & 0 & 0 & g_1 c_{n,0}^\dagger c_{n,4} \\ 0 & 0 & 0 & 0 & 0 & g_2 c_{n,3} c_{n,5}^\dagger \\ 0 & 0 & 0 & 0 & 0 & g_2 c_{n,5} c_{n,3}^\dagger \\ 0 & 0 & 0 & 0 & 0 & 1 \end{pmatrix}. \tag{A4}$$

2. Error bar estimation

We represent the eigenstates of $H = H_0 + H_{3450}$ by matrix product states (MPS, bond dimension $\chi_{\rm MPS}$) and carry out the tensor network DMRG algorithm [48] to variationally determine the ground state and the first few excited states. (We used the TeNPy Library [49] for these calculations.) We impose anti-periodic boundary conditions on the lattice of size L, with L even to avoid the pole in the tangent dispersion at the Brillouin zone boundary.

While the matrix product representation of the Hamiltonian is exact, with small bond dimension $\chi_{\rm MPO}$, the wave function cannot be exactly represented by a matrix product of finite bond dimension $\chi_{\rm MPS}$. We therefore carry out the DMRG calculation at several values of $\chi_{\rm MPS} = 2^p$, increasing in powers of two, and extrapolate to estimate the $\chi_{\rm MPS} \to \infty$ limit of the excitation

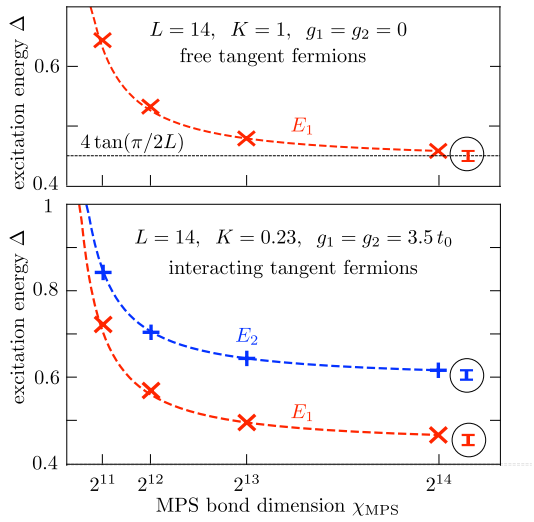

FIG. 5. Dependence of the excitation energies on the MPS bond dimension $\chi_{\rm MPS}$ in the DMRG calculation. The encircled error bars of the $\chi_{\rm MPS} \to \infty$ limit are obtained by the procedure explained in the text. The upper edge of the error bar is aligned with the energy at the largest bond dimension, the lower edge of the error bar is the extrapolation of the fit (A5). The upper panel, for the noninteracting case (when $E_1 = E_2$), is a test to show that the error bars bracket the exact value $4\tan(\pi/2L)$ of the energy of the first excited state.

energies E_n.

The error bars of this extrapolation are estimated as follows, based on two empirical observations:

- Firstly, we find that the calculated $E_n(\chi_{\rm MPS})$ decays monotonically with increasing $\chi_{\rm MPS}$. We therefore align the upper edge of the error bar with the energy at the largest available bond dimension $\chi_{\rm MPS} = 2^{p_{\rm max}}$.

- Secondly, we find that a fit

$$E_n(\chi_{\rm MPS}) = E_n + a_n\,\chi_{\rm MPS}^{-\alpha_n} \tag{A5}$$

to four subsequent values of $\chi_{\rm MPS}$ gives a monotonically increasing fit parameter E_n as larger and larger bond dimensions are included in the fit. We therefore align the lower edge of the error bar with the fit up to $2^{p_{\rm max}}$.

Figure 5 illustrates this procedure, both for the interacting case and for the case of free tangent fermions. The latter case is a test, we can compare with the known value of the excitation energy [$E_1 = 4\tan(\pi/2L)$, an excitation from $-2\tan(\pi/2L)$ to $+2\tan(\pi/2L)$], which is properly bracketed by the error bar.

[1] G. Giuliani and G. Vignale, *Quantum Theory of the Electron Liquid* (Cambridge, 2008).
[2] E. Fradkin, *Field Theories of Condensed Matter Physics* (Cambridge, 2013).
[3] E. Witten, *Three Lectures on Topological Phases of Matter*, Rivista Nuovo Cimento **39**, 313 (2016).
[4] H. J. Rothe, *Lattice Gauge Theories: an Introduction* (World Scientific, 2005).
[5] D. B. Kaplan, *Chiral Symmetry and Lattice Fermions*, Lecture Notes of the Les Houches Summer School, vol. 93 (Oxford, 2009).
[6] D. Tong, *Lectures on Gauge Theory*, `https://www.damtp.cam.ac.uk/user/tong/gaugetheory.html`
[7] P. W. Anderson, *Higgs, Anderson and all that*, Nature Phys. **11**, 93 (2015).
[8] E. Eichten and J. Preskill, *Chiral gauge theories on the lattice*, Nucl. Phys. B **268**, 179 (1986).
[9] Yi-Zhuang You, Yin-Chen He, Cenke Xu, and Ashvin Vishwanath, *Symmetric fermion mass generation as deconfined quantum criticality*, Phys. Rev. X **8**, 011026 (2018).
[10] Juven Wang and Yi-Zhuang You, *Symmetric mass generation*, Symmetry **14**, 1475 (2022).
[11] D. Tong, *Comments on Symmetric Mass Generation in 2d and 4d*, JHEP **07**, 001 (2022).
[12] G. 't Hooft, *Naturalness, chiral symmetry, and spontaneous chiral symmetry breaking*, NATO Sci. Ser. B **59**, 135 (1980).
[13] Juven Wang and Xiao-Gang Wen, *Solution to the (1+1)-dimensional gauged chiral fermion problem*, Phys. Rev. D **99**, 111501 (2019).
[14] Juven Wang and Xiao-Gang Wen, *Non-perturbative regularization of (1+1)-dimensional anomaly-free chiral fermions and bosons: On the equivalence of anomaly matching conditions and boundary gapping rules*, Phys. Rev. B **107**, 014311 (2023).
[15] Meng Zeng, Zheng Zhu, Juven Wang, and Yi-Zhuang You, *Symmetric mass generation in the (1+1)-dimensional chiral fermion 3–4–5–0 model*, Phys. Rev. Lett. **128**, 185301 (2022).
[16] H. B. Nielsen and M. Ninomiya, *A no-go theorem for regularizing chiral fermions*, Phys. Lett. B **105**, 219 (1981).
[17] D.-C. Lu, M. Zeng, J. Wang and Y.-Z. You, *Fermi surface symmetric mass generation*, Phys. Rev. B **107**, 195133 (2023).
[18] R. Thorngren, J. Preskill, and L. Fidkowski, *Chiral lattice gauge theories from symmetry disentanglers*, arXiv:2601.04304.
[19] S. Seifnashri, *Exactly solvable 1+1d chiral lattice gauge theories*, arXiv:2601.14359.
[20] M. DeMarco and X.-G. Wen, *Lattice realization of compact $U(1)$ Chern-Simons theory with exact 1-symmetries*, Phys. Rev. Lett. **126**, 021603 (2021).
[21] L. Fazza and T. Sulejmanpasic, *Lattice quantum Villain Hamiltonians: Compact scalars, $U(1)$ gauge theories, fracton models and quantum Ising model dualities*, JHEP **05**, 017 (2013).
[22] Z. Lu, S. Seifnashri, and S.-H. Shao, *Lattice chiral symmetry from bosons in 3+1d*, arXiv:2604.06307.
[23] L. Fidkowski, C. Xu, and C. Zhang, *Non-invertible bosonic chiral symmetry on the lattice*, arXiv:2510.17969.
[24] E. Berkowitz, A. Cherman, and T. Jacobson, *Ex-*

act lattice chiral symmetry in 2d gauge theory, arXiv:2310.17539.

[25] R. Stacey, *Eliminating lattice fermion doubling*, Phys. Rev. D **26**, 468 (1982).

[26] V. A. Zakharov, J. Tworzydło, C. W. J. Beenakker, and M. J. Pacholski, *Helical Luttinger liquid on a space-time lattice*, Phys. Rev. Lett. **133**, 116501 (2024).

[27] J. Haegeman, L. Lootens, Q. Mortier, A. Stottmeister, A. Ueda, and F. Verstraete, *Interacting chiral fermions on the lattice with matrix product operator norms*, arXiv:2405.10285

[28] V. A. Zakharov, S. Polla, A. Donís Vela, P. Emonts, M. J. Pacholski, J. Tworzydło, and C. W. J. Beenakker, *Luttinger liquid tensor network: Sine versus tangent dispersion of massless Dirac fermions*, Phys. Rev. Res. **6**, 043059 (2024).

[29] V. A. Zakharov, J. Sánchez Fernán, and C. W. J. Beenakker, *Lattice fermion simulation of spontaneous time-reversal symmetry breaking in a helical Luttinger liquid*, Annalen Physik **538**, e00004 (2026).

[30] M. J. Pacholski, G. Lemut, J. Tworzydło, and C. W. J. Beenakker, *Generalized eigenproblem without fermion doubling for Dirac fermions on a lattice*, SciPost Phys. **11**, 105 (2021).

[31] C. W. J. Beenakker, A. Donís Vela, G. Lemut, M. J. Pacholski, and J. Tworzydło, *Tangent fermions: Dirac or Majorana fermions on a lattice without fermion doubling*, Annalen Physik **535**, 2300081 (2023).

[32] F. D. M. Haldane, *Stability of chiral Luttinger liquids and Abelian quantum Hall states*, Phys. Rev. Lett. **74**, 2090 (1995).

[33] Y.-M. Lu and A. Vishwanath, *Theory and classification of interacting integer topological phases in two dimensions: A Chern-Simons approach*, Phys. Rev. B **86**, 125119 (2012).

[34] M. Levin, *Protected edge modes without symmetry*, Phys. Rev. X **3**, 021009 (2013).

[35] Juven Wang and Xiao-Gang Wen, *Boundary degeneracy of topological order*, Phys. Rev. B **91**, 125124 (2015).

[36] T. Giamarchi, *Quantum Physics in One Dimension* (Clarendon Press, Oxford, 2003).

[37] G. Dolcetto, M. Sassetti, T. L. Schmidt, *Edge physics in two-dimensional topological insulators*, Rivista del Nuovo Cimento **39**, 113 (2016).

[38] P. Boyle Smith and D. Tong, *Boundary states for chiral symmetries in two dimensions*, J. High Energy Phys. **09**, 018 (2020).

[39] A. Yegulalp, *Fermions coupled to a conformal boundary: A generalization of the monopole-fermion system*, Phys. Lett. B **328**, 379 (1994).

[40] M. van Beest, P. Boyle Smith, D. Delmastro, Z. Komargodski, and D. Tong, *Monopoles, scattering, and generalized symmetries*, J. High Energy Phys. **03**, 014 (2025).

[41] L. P. Kadanoff, *Multicritical behavior at the Kosterlitz-Thouless critical point*, Ann. Phys. **120**, 39 (1979).

[42] S.-I. Tomonaga, *Remarks on Bloch's method of sound waves applied to many-fermion problems*, Prog. Theor. Phys. **5**, 544 (1950).

[43] J. M. Luttinger, *An exactly soluble model of a many-fermion system*, J. Math. Phys. **4**, 1154 (1963).

[44] The single-connectedness argument of Sec. IV C carries through if the minimum of the cosine potential is not at zero, because the translation on the torus is a continuous deformation that preserves all topological properties, including connectedness.

[45] D. Cox, J. Little, and H. Schenck, *Toric Varieties* (American Mathematical Soc., 2011). The gcd condition for a singly-connected kernel of the map $\mathcal{A}$ can be equivalently stated as a condition on the Smith normal form of the integer matrix A: The invariant factors should all be equal to unity.

[46] As an example of a non-primitive set of interaction vectors, we note $\boldsymbol{\ell}^{(1)} = (1, 3, -3, 1)$, $\boldsymbol{\ell}^{(2)} = (-3, 1, 1, 3)$. These satisfy the conditions (2.4) and (2.5), but they do not span a primitive lattice: The fractional linear combination $\boldsymbol{L} = \frac{1}{2}\boldsymbol{\ell}^{(1)} + \frac{1}{2}\boldsymbol{\ell}^{(2)} = (-1, 2, -1, 2)$ defines a local vertex operator $\mathcal{O} = e^{i\boldsymbol{L}\Phi}$ that can distinguish inequivalent pinned bosonic fields: If $\cos(\boldsymbol{\ell}^{(p)}\Phi) = 2\pi n_p$, then $\mathcal{O} = (-1)^{n_1+n_2}$ takes on the value ± 1 on the two inequivalent minima of the cosine potential.

[47] B. Pirvu, V. Murg, J.I. Cirac and F Verstraete, *Matrix product operator representations*, New J. Phys. **12**, 025012 (2010).

[48] U. Schollwöck, *The density-matrix renormalization group in the age of matrix product states*, Annals Physics **326**, 96 (2011).

[49] J. Hauschild and F. Pollmann *Efficient numerical simulations with Tensor Networks: Tensor Network Python (TeNPy)*, SciPost Phys. Lect. Notes **5** (2018).